View metadata, citation and similar papers at core.ac.uk
brought to you by CORE
provided by Tomsk State University Repository

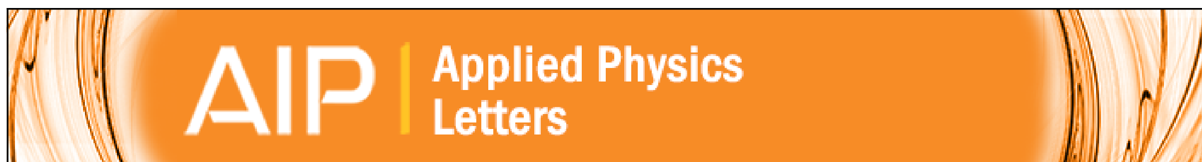

Phonon bottleneck in p-type Ge/Si quantum dots

A. I. Yakimov, V. V. Kirienko, V. A. Armbrister, A. A. Bloshkin, and A. V. Dvurechenskii

Citation: Applied Physics Letters **107**, 213502 (2015); doi: 10.1063/1.4936340
View online: http://dx.doi.org/10.1063/1.4936340
View Table of Contents: http://scitation.aip.org/content/aip/journal/apl/107/21?ver=pdfcov
Published by the AIP Publishing

Articles you may be interested in
Effect of overgrowth temperature on the mid-infrared response of Ge/Si(001) quantum dots
Appl. Phys. Lett. **100**, 053507 (2012); 10.1063/1.3682304

Gigantic uphill diffusion during self-assembled growth of Ge quantum dots on strained SiGe sublayers
Appl. Phys. Lett. **96**, 141909 (2010); 10.1063/1.3383241

Molecular epitaxy and the electronic properties of Ge/Si heterosystems with quantum dots
Low Temp. Phys. **30**, 877 (2004); 10.1063/1.1820017

Near-infrared waveguide photodetector with Ge/Si self-assembled quantum dots
Appl. Phys. Lett. **80**, 509 (2002); 10.1063/1.1435063

Diffusional narrowing of Ge on Si(100) coherent island quantum dot size distributions
Appl. Phys. Lett. **71**, 614 (1997); 10.1063/1.119809

AIP APL Photonics
APL Photonics is pleased to announce
Benjamin Eggleton as its Editor-in-Chief

This article is copyrighted as indicated in the article. Reuse of AIP content is subject to the terms at: http://scitation.aip.org/termsconditions. Downloaded to IP: 84.237.80.170 On: Tue, 24 Nov 2015 02:23:14

APPLIED PHYSICS LETTERS 107, 213502 (2015)

Phonon bottleneck in *p*-type Ge/Si quantum dots

A. I. Yakimov,[1,2,a)] V. V. Kirienko,[1] V. A. Armbrister,[1] A. A. Bloshkin,[1,3] and A. V. Dvurechenskii[1,3]
[1]*Rzhanov Institute of Semiconductor Physics, Siberian Branch of the Russian Academy of Science, 630090 Novosibirsk, Russia*
[2]*Tomsk State University, 634050 Tomsk, Russia*
[3]*Novosibirsk State University, 630090 Novosibirsk, Russia*

(Received 17 June 2015; accepted 6 November 2015; published online 23 November 2015)

We study the effect of quantum dot size on the mid-infrared photo- and dark current, photoconductive gain, and hole capture probability in ten-period *p*-type Ge/Si quantum dot heterostructures. The dot dimensions are varied by changing the Ge coverage and the growth temperature during molecular beam epitaxy of Ge/Si(001) system in the Stranski-Krastanov growth mode. In all samples, we observed the general tendency: with decreasing the size of the dots, the dark current and hole capture probability are reduced, while the photoconductive gain and photoresponse are enhanced. Suppression of the hole capture probability in small-sized quantum dots is attributed to a quenched electron-phonon scattering due to phonon bottleneck. © *2015 AIP Publishing LLC*.
[http://dx.doi.org/10.1063/1.4936340]

Quantum dot (QD) infrared photodetectors (QDIPs) are operated in a similar manner as quantum well (QW) infrared photodetectors. The only difference is that the carriers in a QDIP are confined in all three dimensions. However, it is well known that QDIPs have several important advantages over QW devices.[1,2] One figure of merit that determines the photoconductive gain and hence the QDIP responsivity is the probability that a carrier is captured by a QD after its optical generation. A remarkable property of QDs originated from their discrete energy spectrum is a suppression of carrier relaxation rates due to the phonon bottleneck effect.[3,4] If the energy separation between discrete quantized levels in the dot is designed such that it exceeds the energy of optical phonons, then the electron-phonon scattering becomes strongly quenched leading to a long carrier relaxation time. A reduced capture probability of photoexcited carriers will result in enhancement of the photoconductive gain and detector response.[5] Clearly, this effect can be particularly important in heterostructures with small QDs having markedly separated bound states.

The phonon bottleneck has been proposed for electrons[3,4] and observed experimentally for undoped[6–9] and *n*-type QDs[10,11] using photoluminescence spectroscopy or pump-probe technique. So far, little attention has been paid to QDIPs with *p*-type hole response. The attractive features of *p*-QDIPs include a well-preserved spectral profile,[12] as an opposite to a conventional *n*-type response strongly dependent on the applied bias, increased density of states, and lower dark current due to the higher hole effective mass.[13] All these features have motivated the study the hole capture process in *p*-type QDs. The work described here focuses on the Ge/Si(001) system. The 4% lattice mismatch between the Ge epitaxial film and the Si is used to induce the Stranski-Krastanov growth mode where the two-dimensional growth characteristic changes into a three-dimensional one after the deposition of about 4.5 monolayers of Ge. The Ge/Si QDIPs operate in the mid-infrared atmospheric window by photoexcitation of holes out of Ge QDs into the continuum above the Si barriers and subsequent transportation by an internal or built-in electric field.[14–19] To trace the phonon bottleneck effect, we compare the detailed measurements of the intraband photocurrent, dark current, photoconductive gain, and the hole capture probability of three Ge/Si QDIPs with Ge dots of different sizes.

Figure 1(a) shows schematically the structure of the devices discussed in this paper. The samples were grown by solid source molecular beam epitaxy on a (001) oriented boron doped p^+-Si substrate with resistivity of 0.01 Ω cm. The active region of the devices was composed of ten stacks of Ge quantum dots separated by 35-nm Si barriers. The large QDs were fabricated by deposition of Ge layers with a nominal coating thickness of 6.5 monolayers at a temperature of 620 °C. Atomic force microscopy (AFM) and scanning tunneling microscopy (STM) of samples without the Si cap layers were employed to assess the morphology of the Ge surface. The dots have the shape of a lens or a dome with a circular base.[20] The typical dot height is 18 nm and their base diameter is around 84 nm with the standard deviation ±5%. The QD areal density is $3 \times 10^9\ \mathrm{cm}^{-2}$ (Fig. 1(d)). Two other samples were grown at a lower temperature of 500 °C. To obtain QDs with medium size, each Ge layer was formed subsequently by depositing 7 monolayers of pure Ge. To synthesize small Ge dots, the Ge growth in each layer was stopped just after appearance of well-defined three-dimensional spots in the reflection high-energy electron diffraction pattern. After the deposition at 500 °C, hut shaped Ge islands are observed (Figs. 1(b) and 1(c)). The medium-sized Ge dots have a typical base length $\langle l \rangle = 18.2 \pm 3.1$ nm (Fig. 1(f)), about 2 nm height, and an areal density of $1.1 \times 10^{11}\ \mathrm{cm}^{-2}$. For small dots, $\langle l \rangle = 10.8 \pm 1.6$ nm (Fig. 1(e)), ~1 nm height, and a slightly larger density of $1.3 \times 10^{11}\ \mathrm{cm}^{-2}$. The active region was sandwiched in between the 200-nm-thick intrinsic Si buffer and cap layers. Finally, a boron doped 200-nm-thick p^+-Si top contact layer was deposited. The *p*-type remote

[a)]yakimov@isp.nsc.ru

This article is copyrighted as indicated in the article. Reuse of AIP content is subject to the terms at: http://scitation.aip.org/termsconditions. Downloaded to IP: 84.237.80.170 On: Tue, 24 Nov 2015 02:23:14

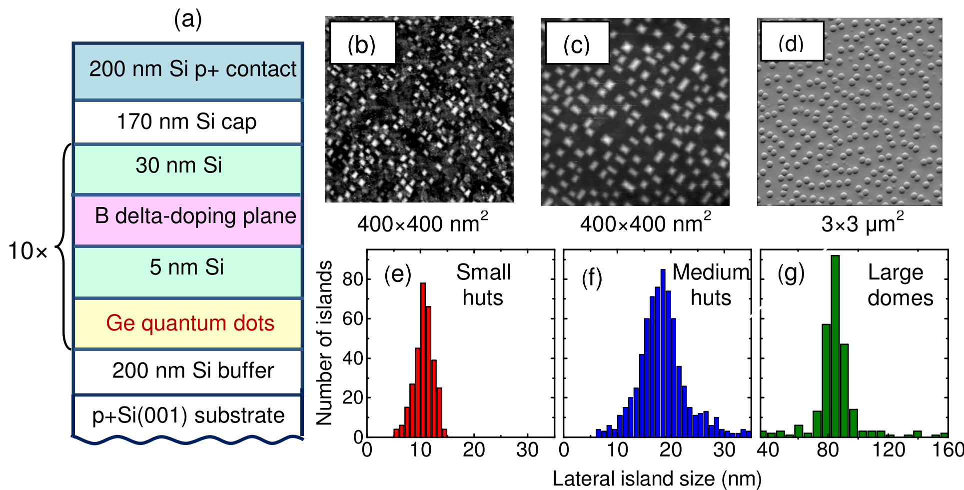

FIG. 1. (a) Layer sequence of the Ge/Si heterostructures. STM images [(b) and (c)], AFM image (d), and size distribution histograms [(e)–(g)] from topmost uncapped Ge layer of small-dot [(b) and (e)], medium-dot [(c) and (f)], and large-dot [(d) and (g)] samples. The image size is $400 \times 400\,\text{nm}^2$ in (b) and (c), and $3 \times 3\,\mu\text{m}^2$ in (d).

doping of the dots was achieved with a boron δ-doping layer inserted 5 nm above each dotted layer. The areal doping density ($0.8 \times 10^{12}\,\text{cm}^{-2}$) was the same for all three samples. The Si barriers were deposited at 500 °C. At the chosen growth conditions, the exponential decay length of B delta doping profiles in growth direction is less than 1 nm,[21] so that the boron atoms do not reach the dot layers. Due to Si diffusion, the obtained dots are not pure Ge. The average Ge content of $x = 0.43$ in large QDs, 0.61 in QDs with intermediate sizes, and 0.65 in small QDs was determined from Raman scattering experiments (Fig. 2) using an approach described in Ref. 22.

For vertical photocurrent (PC) measurements, the samples were processed in the form of circular mesas with diameter 4.5 mm by using plasma etching and contacted by Al:Si metallization (the Al/Si spots are about 1 mm in diameter). The bottom contact is defined as the ground when applying voltage to the detectors. The normal-incidence photoresponse was obtained using a Bruker Vertex 70 Fourier transform infrared (FTIR) spectrometer with a spectral resolution of $10\,\text{cm}^{-1}$ along with a SR570 low noise current preamplifier. The PC spectra were calibrated with a deuterated L-alanine doped triglycine sulfate (DLaTGS) detector. The noise characteristics were measured with an SR770 fast Fourier transform analyzer and the white noise region of the spectra was used to determine the gain. The sample noise was obtained by subtracting the preamplifier-limited noise level from the experimental data. The dark current was tested as a function of bias (U_b) by a Keithley 6430 Sub-Femtoamp Remote SourceMeter. The devices were mounted in a cold finger inside a Specac cryostat with ZnSe windows. For dark current and noise measurements, the samples were surrounded with a cold shield. All measurements were carried out at a temperature of 80 K.

The dark current-voltage characteristics of three samples are shown in Fig. 3. The dark current is substantially lower in the device with smallest QDs due to the reduced overlap of the zero-dimensional density of states with the Fermi function and suppression of thermoionic emission from the thermally populated excited states.[1] Figure 4 depicts the PC spectra measured at a zero bias voltage. All QDIPs show pronounced photovoltaic behavior caused by a built-in electric field of charged δ-doping planes.[19,23] The broad nature of the photoresponse suggests that the photocurrent is associated with a bound-to-continuum transition.[19,24–26] As the dot size decreases, the peak position shifts toward less photon energy by ~100 meV. This property follows directly from the general properties of quantum dots: decreasing the dot dimensions will reduce the hole binding energies getting them closer to the continuum states.[27] We find that the PC for small dots integrated over the mid-infrared atmospheric window from 3 to 5 μm

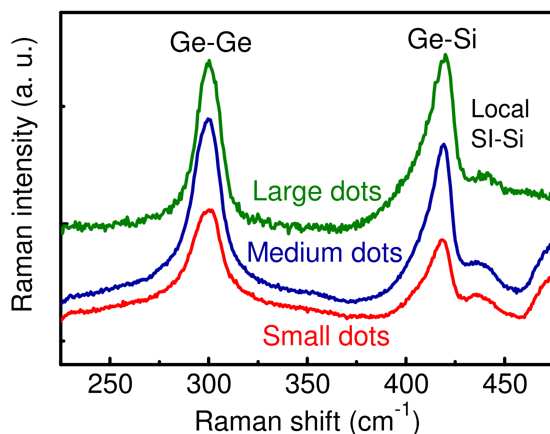

FIG. 2. Raman spectra of the samples under study in the frequency range of optical vibrations of Ge–Ge and Ge–Si bonds.

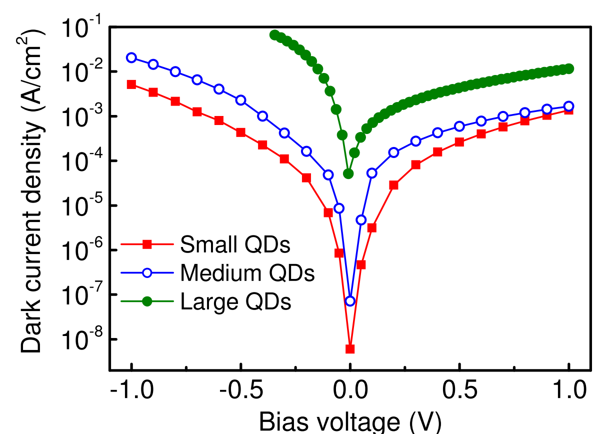

FIG. 3. The dark current density measured as a function of bias for Ge/Si QDIPs at $T = 80$ K.

This article is copyrighted as indicated in the article. Reuse of AIP content is subject to the terms at: http://scitation.aip.org/termsconditions. Downloaded to IP: 84.237.80.170 On: Tue, 24 Nov 2015 02:23:14

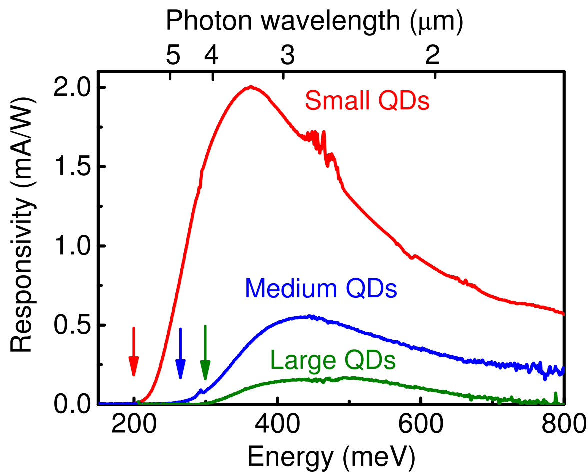

FIG. 4. Zero-bias photoresponse measured for samples with QDs of different sizes. The arrows indicate the calculated ground-state hole binding energies.

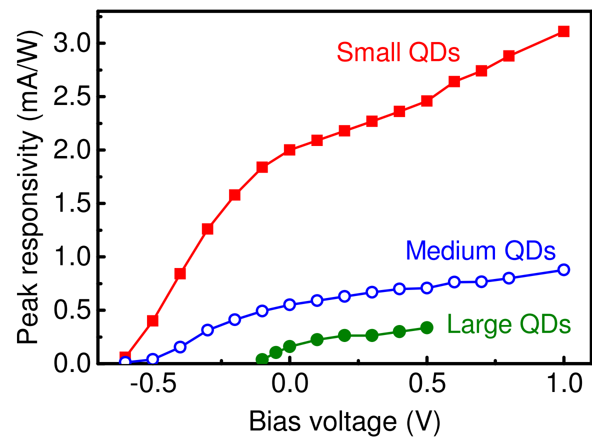

FIG. 5. Peak responsivity as a function of applied bias. The data were taken at 363 meV for the sample with small QDs, at 432 meV for QDIP with medium dot dimensions, and at 493 meV for the large-dot device. For the large QDs, at biases just above 0.5 V, the signal becomes too noise to detect PC.

exceeds the signals from medium and large QDs by factors of about 8 and 32, respectively.

In order to support the origin of the photoresponse, we performed a three-dimensional analysis of the valence band diagram for the samples under study. We took for our modeling two different island shapes typically observed in our samples: a Ge_xSi_{1-x} pyramid with {105}-oriented facets and a Ge_xSi_{1-x} lens. Note that the pyramid is a particular case of a hut shaped cluster with a square base. The dot sizes and composition were taken from the experiment. The pyramid or lens lie on a thin Ge_xSi_{1-x} wetting layer and are embedded into the Si matrix. The finite element calculations of three-dimensional spatial distribution of strain components $\varepsilon_{\alpha\beta}$ were performed using the package COMSOL Multiphysics with the approach described in Ref. 28. The strain tensor elements were subsequently used as input to a strain-dependent Hamiltonian. The hole energy spectra were calculated with a six-band $\mathbf{k}\cdot\mathbf{p}$ approximation (three valence bands and spin), based on the method of Bir and Pikus,[29] includes spin-orbit and strain effects. Details of the model and formulation can be found in Ref. 30. From theoretical analysis, we found that the ground hole state is located about 303, 272, and 202 meV from the Si barrier edge for the large-dot, medium-dot, and small-dot samples, respectively. All these values agree well with the onset of the photoresponse shown by arrows in Fig. 4. Thus, the observed photocurrent is associated with the dominant transitions from the ground state within the Ge dots to continuum states at the Si valence band edge. Possible optical excitations from the other bound states have much smaller oscillator strength due to the presence of the nodal planes in wavefunction density and make a small contribution to PC.

Figure 5 compares the peak responsivity R of the devices, which shows a significant improvement of R over the wide bias range: the peak photoresponse of the sample with small dots is found to be about 4 times higher than that of the medium-dot sample with the same dot density and by an order larger than in the large-dot device. Asymmetry of $R(U_b)$ dependence with respect to zero bias is a typical feature of Ge/Si QDIPs with a remote delta-doping of Si barriers and has been discussed in detail in Ref. 19. Responsivity is given by $R=(e\lambda/hc)\eta g$, where c is the speed of light, η is the absorption quantum efficiency, and g is the photoconductive gain defined as the ratio of the photocarrier lifetime over the transit time. Since the doping level, dot density, and the shape of QDs are the same at least in two QDIPs containing huts, we suggest that the rise of R is primarily due to the increasing photoconductive gain.

From noise measurements, we established that the noise level at finite bias is dominated by a generation-recombination noise. As it has been demonstrated by Ershov and Liu[31] and experimentally verified by Schönbein *et al.*,[32] when the carrier capture probability into a QW is much smaller than unity, the photoconductive gain and the noise gain are equal and can be found from

$$g = i_n^2/(4eI_d\Delta f), \tag{1}$$

where e is the charge of an electron, i_n is the noise current, I_d is the dark current, and Δf is the noise bandwidth. Ye *et al.*[33] assumed that since QDIPs have similar layer structure to that of QWIPs, the charge transport mechanisms of the QDIPs are similar to those of QWs, except that the fill factor of quantum dot layers is less than unity. In this case, the gain can be expressed in terms of the capture probability of an electron (or hole) traversing a QD layer p_c as[33]

$$g = \frac{1-p_c/2}{FNp_c}, \tag{2}$$

where F is the fill factor which describes the area coverage of the QDs in a dot layer, N is the number of QD layers. The fill factor of 0.16, 0.35, and 0.17 was estimated from the STM and AFM data presented in Figures 1(b), 1(c), and 1(d), respectively. For the evaluation of the gain, we have subtracted the thermal (Johnson) noise from the measured noise in order to have the pure generation-recombination noise. The Johnson noise was calculated as $i_J=\sqrt{4kT\Delta f/\rho}$, where k is the Boltzmann's constant, T is the temperature, and ρ is the differential resistance, which is extracted from the dark current measurements.

The gain and hole capture probability calculated using Eqs. (1) and (2) are shown in Figure 6. The data near zero

This article is copyrighted as indicated in the article. Reuse of AIP content is subject to the terms at: http://scitation.aip.org/termsconditions. Downloaded to IP: 84.237.80.170 On: Tue, 24 Nov 2015 02:23:14

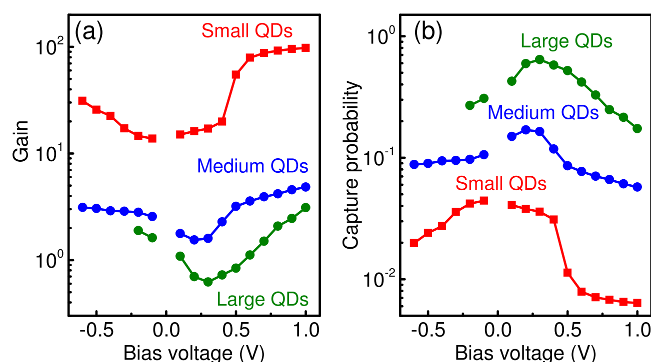

FIG. 6. Photoconductive gain (a) and hole capture probability (b) as a function of applied bias.

bias has been omitted since the values are artificially high due to the very low dark current. For the sample with small QDs, the gain is much higher than unity and the capture probability is small displaying a suppression factor of 3–30 depending on applied voltage and dot size. Reduction of the hole capture probability, enhancement of photocurrent and the gain with the decrease of the dot dimensions can be explained if we assume a phonon bottleneck effect for holes. A carrier optically excited from the ground state to the continuum is first captured to the higher-laying excited states of the QD and then go down in energy towards the ground state. The smaller splitting between levels the faster relaxation. Since the energy separation of confined states increases with decreasing the quantum state number,[34] it is reasonable to expect that the step, which inhibits the overall relaxation process, is a final transition between the lowest two states. The calculated energy gaps between the ground and the first excited state are $\Delta E = 37$ and 60 meV for the samples containing medium and small QDs, respectively. In a device with largest dots, $\Delta E = 0.4$ meV. The energy level spacing for the small Ge dots exceeds all LO phonon energies corresponding to Si–Si (54 meV), Si–Ge (52 meV), and Ge–Ge (37 meV) vibrations (Fig. 2) and therefore holes can display an effective bottleneck in the relaxation towards the ground state due to the lack of phonons needed to satisfy the energy conservation rule. An opposite energy ratio is observed for QDs with intermediate dimensions where the Si–Si and Si–Ge phonon energies are larger than ΔE and the Ge–Ge energy is very close to ΔE. In this case, the single-phonon mediated scattering process is allowed due to the interaction with a Ge–Ge vibration mode, and in agreement with the experimental observations. In a large-dot device, the hole spectrum has a QW-like character with a quasi-two-dimensional density of states, and the relaxation between the discrete eigenstates can be fast due to the presence of a great number of suitable final states.

In summary, we have studied the impact of QD size on the photoelectrical characteristics of *p*-type Ge/Si quantum-dot heterostructures. In particular, we obtain an improvement of the peak responsivity by one order of magnitude by enhancing the photoconductive gain due to the phonon bottleneck, which we realize by reducing the dot dimensions. Our results indicate that a proper choice of QD size can serve as a promising way to optimize the Ge/Si QDIP performance.

The authors are much obliged to V. A. Volodin for Raman measurements and to P. A. Kuchinskaya and A. A. Shklyaev for AFM and STM experiments, respectively. The work was funded by Russian Scientific Foundation (Grant No. 14-12-00931).

[1]V. Ryzhii, Semicond. Sci. Technol. **11**, 759 (1996).
[2]J. Phillips, J. Appl. Phys. **91**, 4590 (2002).
[3]U. Bockelmann and G. Bastard, Phys. Rev. B **42**, 8947 (1990).
[4]H. Benisty, C. M. Sotomayor-Torrés, and C. Weisbuch, Phys. Rev. B **44**, 10945 (1991).
[5]V. Ryzhii, I. Khmyrova, V. Pipa, V. Mitin, and M. Willander, Semicond. Sci. Technol. **16**, 331 (2001).
[6]R. Heitz, H. Born, F. Guffarth, O. Stier, A. Schliwa, A. Hoffman, and D. Bimberg, Phys. Rev. B **64**, 241305 (2001).
[7]T. Kitamura, R. Ohtsubo, M. Murayyama, T. Kuroda, K. Yamaguchi, and A. Tackeuchi, Phys. Status Solidi C **0**, 1165 (2003).
[8]J. Urayama, T. B. Norris, J. Singh, and P. Bhattachara, Phys. Rev. Lett. **86**, 4930 (2001).
[9]G. Reithmaier, F. Flassig, P. Hasch, S. Lichtmannecker, K. Müller, J. Vŭcković, R. Gross, M. Kaniber, and J. J. Finley, Appl. Phys. Lett. **105**, 081107 (2014).
[10]S. Sauvage, P. Boucaud, R. P. S. M. Lobo, F. Bras, G. Fishman, R. Prazeres, F. Glotin, J. M. Ortega, and J.-M. Gérard, Phys. Rev. Lett. **88**, 177402 (2002).
[11]E. A. Zibik, L. R. Wilson, R. P. Green, G. Bastard, R. Ferreira, P. J. Phillips, D. A. Carder, J.-P. R. Wells, J. W. Cockburn, M. S. Skolnick, M. J. Steer, and M. Hopkinson, Phys. Rev. B **70**, 161305(R) (2004).
[12]Y.-F. Lao, S. Wolde, A. G. Unil Perera, Y. H. Zhang, T. M. Wang, J. O. Kim, T. Schuler-Sandy, Z.-B. Tian, and S. S. Krishna, Appl. Phys. Lett. **104**, 171113 (2014).
[13]Y.-F. Lao, S. Wolde, A. G. Unil Perera, Y. H. Zhang, T. M. Wang, H. C. Liu, J. O. Kim, T. Schuler-Sandy, Z.-B. Tian, and S. S. Krishna, Appl. Phys. Lett. **103**, 241115 (2013).
[14]C. Miesner, O. Röthig, K. Brunner, and G. Abstreiter, Appl. Phys. Lett. **76**, 1027 (2000).
[15]D. Bougeard, K. Brunner, and G. Abstreiter, Phys. E (Amsterdam) **16**, 609 (2003).
[16]C.-H. Lin, C.-Y. Yu, C.-Y. Peng, W. S. Ho, and C. W. Liu, J. Appl. Phys. **101**, 033117 (2007).
[17]E. Finkman, N. Shuall, A. Vardi, V. Le Thanh, and S. E. Schacham, J. Appl. Phys. **103**, 093114 (2008).
[18]R. K. Singha, S. Manna, S. Das, A. Dhar, and S. K. Ray, Appl. Phys. Lett. **96**, 233113 (2010).
[19]A. I. Yakimov, V. A. Timifeev, A. A. Bloshkin, V. V. Kirienko, A. I. Nikiforov, and A. V. Dvurechenskii, J. Appl. Phys. **112**, 034511 (2012).
[20]A. I. Yakimov, V. V. Kirienko, A. A. Bloshkin, V. A. Armbrister, P. A. Kuchinskaya, and A. V. Dvurechenskii, Appl. Phys. Lett. **106**, 032104 (2015).
[21]H. Jorke and H. Kibbel, Appl. Phys. Lett. **57**, 1763 (1990).
[22]A. I. Yakimov, A. I. Nikiforov, A. V. Dvurechenskii, V. V. Ulyanov, V. A. Volodin, and R. Groetzschel, Nanotechnology **17**, 4743 (2006).
[23]L. Chu, A. Zrenner, G. Böhm, and G. Abstreiter, Appl. Phys. Lett. **75**, 3599 (1999).
[24]D. Pan, E. Towe, and S. Kennerly, Appl. Phys. Lett. **73**, 1937 (1998).
[25]W. Q. Ma, X. J. Yang, M. Chong, T. Yang, L. H. Chen, J. Shao, X. Lü, W. Lu, C. Y. Song, and H. C. Liu, Appl. Phys. Lett. **93**, 013502 (2008).
[26]A. D. Stiff, S. Krishna, P. Bhattacharya, and S. Kennerly, Appl. Phys. Lett. **79**, 421 (2001).
[27]N. A. Ameen and Y. M. El-Batawy, J. Appl. Phys. **113**, 193102 (2013).
[28]M. A. S. Christiansen and H. P. Strunk, Appl. Phys. Lett. **64**, 3617 (1994).
[29]G. L. Bir and G. E. Pikus, *Symmetry and Strain-Induced Effects in Semiconductors* (Wiley, New York, 1974).
[30]A. I. Yakimov, A. A. Bloshkin, and A. V. Dvurechenskii, Phys. Rev. B **81**, 115434 (2010).
[31]M. Ershov and H. C. Liu, J. Appl. Phys. **86**, 6580 (1999).
[32]C. Schönbein, H. Schneider, R. Rehm, and M. Walther, Appl. Phys. Lett. **73**, 1251 (1998).
[33]Z. Ye, J. C. Campbell, Z. Chen, E. T. Kim, and A. Madhukar, Appl. Phys. Lett. **83**, 1234 (2003).
[34]A. I. Yakimov, A. V. Dvurechenskii, and A. I. Nikiforov, J. Nanoelectron. Optoelectron. **1**, 119 (2006).

This article is copyrighted as indicated in the article. Reuse of AIP content is subject to the terms at: http://scitation.aip.org/termsconditions. Downloaded to IP: 84.237.80.170 On: Tue, 24 Nov 2015 02:23:14